ULTRASONIC TRANSDUCER RADIATION THROUGH A CURVED FLUID-SOLID INTERFACE

Terence P. Lerch and Lester W. Schmerr
Center for NDE and the Department of Aerospace
Engineering and Engineering Mechanics
Iowa State University
Ames, Ia 50011

Alexander Sedov
Department of Mechanical Engineering
Lakehead University
Thunder Bay, Ontario
Canada P7B 5E1

INTRODUCTION

A number of typical ultrasonic immersion inspections require the transducer radiation to propagate through components with non-planar surfaces. As the complexity of the component's surface increases in terms of shape and curvature, the effects of the part's curvature on the transmitted wavefield become difficult, if not impossible, to predict by simple heuristic approaches. The development of accurate transducer beam models that can handle these types of fluid-solid interfaces, therefore, becomes essential.

Many authors have studied the issue of curved interfaces previously, and have achieved differing degrees of success in modeling the essential physics of the problem. Numerous versions of the Gauss-Hermite beam model [1,2,3] have been implemented in the past, and while they have been successfully used for many inspection situations, they are all inherently restricted by the paraxial approximation. The Boundary Element Method (BEM) [4] is another popular technique used for fluid-solid interface problems, but as the transducer's wavenumber increases, BEM becomes increasingly difficult to implement. The Complex Source Technique (CSP) [5] has also been implemented in the past, but this technique assumes a quasi-gaussian beam profile over the transducer, which fails to capture all of the complexity of the true transducer profile, particularly in the nearfield.

Here, we briefly describe and compare a hierarchy of four transducer beam models and demonstrate their use for simple cylindrical and bicylindrical interface curvatures (see Figure 1a). However, two of these models (KBT and edge element technique) are in fact applicable to arbitrary types of curvatures. The first, and most general, of the models is called the Kirchhoff Beam Transmission (KBT) model. Only Rayleigh-Sommerfeld theory [6] and the Kirchhoff approximation are assumed in its derivation. Unfortunately, its applicability to general geometries comes at the price of having to evaluate two 2-D surface integrals, where one surface integral is associated with the transducer face, and the other with the interface surface. Avoiding or simplifying the numerical evaluation of these two surface integrals is the motivation for considering the other 3 models.

Two different approaches can be taken to aid in the evaluation of the KBT model. First, the edge element technique [7] can be applied directly to the KBT model, effectively reducing the two surface integrals to a series of four, nested finite summations. This model

Review of Progress in Quantitative Nondestructive Evaluation, Vol 17
Edited by D.O. Thompson and D.E. Chimenti, Plenum Press, New York, 1998

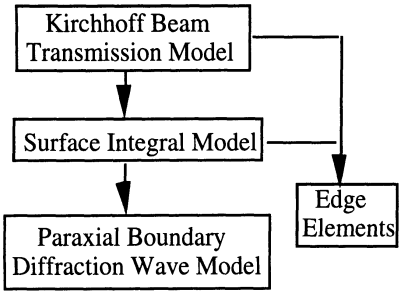

Figure 1a. Hierarchy of beam models for curved interfaces.

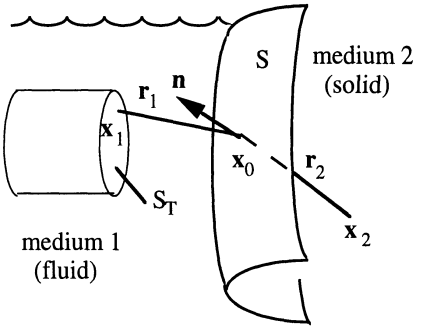

Figure 1b. Beam propagation transmitted through a curved, fluid-solid interface.

is known as the edge element approach. Second, the method of stationary phase can be applied to the interface surface integral of the KBT model, essentially expanding the transmitted wavefield about the stationary phase ray path, and leaving only the 2-D surface integral of the transducer face to be evaluated. This model is called the surface integral (SI) model. Finally, the 2-D integral of the SI model can be simplified further by invoking the paraxial approximation and reducing the 2-D surface integral to a 1-D line integral around the extended contour of the transducer's rim. This model is called the paraxial boundary diffraction wave (PBDW) model. As the integration associated with each of the models is reduced, the computational speed at which the transducer wavefield can be calculated increases dramatically. It should be noted that Schmerr et al. [8] gives a more complete description of the development of each of the particular models.

Here, we briefly introduce the four models and their associated parameters. Next, we compare the on-axis profiles predicted by the edge element and PBDW models for a relatively simple, cylindrical interface problem. Finally, the predicted wavefields of three related geometries will be compared. Cross-axis profiles computed by the edge element technique for planar, filleted, and cylindrically converging interfaces will be shown, along with a 2-D image of the beam profile transmitted through the filleted interface.

CURVED INTERFACE BEAM MODELS

As mentioned in the Introduction, a brief summary of each of the curved interface beam models will be given. The models compute the incident displacement fields discretely at a single spatial point in the second medium (homogeneous, isotropic, elastic solid) for a single, user specified, frequency. A $\exp(-i\omega t)$ time dependency will be suppressed throughout the paper.

The problem under consideration is shown in Figure 1b. A transducer radiates a beam of ultrasound into the fluid which propagates through an interface of general curvature into the underlying elastic solid being interrogated. The incident pressure generated by the transducer in the fluid is described by the Rayleigh-Sommerfeld integral. As shown by O'Neil [6] and others, the Rayleigh-Sommerfeld integral is applicable to focused, as well as unfocused, radiators, provided the focusing is not too "tight".

An integral representation of the displacements in the solid can be written for a point pressure source in the fluid medium. This integral representation will depend on the displacements and their derivatives at the interface, and the fundamental solution for the solid. If the curvature of the interface is assumed to be much greater than the wavelength of the transmitted radiation, we can model the local interaction of the ultrasound at the interface as plane wave impinging on a planar interface, S, (Kirchhoff approximation). For any arbitrary, small patch of interface surface, the displacements and their derivatives at that small

patch can be written in terms of the pressure in the fluid medium. The fundamental solution and its derivative can also be written explicitly at high frequencies. The expressions for the displacements and fundamental solution (and their respective derivatives) can then be substituted into the integral representation, resulting in an explicit equation for the incident displacements propagating in the second medium due to a point source radiating in the first medium. If these point source solutions are integrated over the transducer surface (S_T), the incident displacement field generated by the transducer becomes

$$u_{Tn}^{\gamma}(\mathbf{x}_2,\omega) = \frac{-\rho_1 v_0}{8\pi^2\rho_2}\sum_{\alpha=P,S}\int_{S_T}\left\{\int_S \frac{T_{12}^{\alpha;P}}{c_{\alpha 2}} I_n^{\alpha\gamma}\frac{\exp(ik_{p1}r_1)}{r_1}\frac{\exp(ik_{\gamma 2}r_2)}{r_2}dS(\mathbf{x}_s)\right\}dS(\mathbf{x}_1) \qquad (1)$$

where

$$I_n^{\alpha\gamma} = \frac{1}{\rho_2 c_{\gamma 2}^2} f_{ln}^{\gamma} C_{klij} d_i^{\alpha}\left[ik_{\alpha 2}n_k e_j^{\alpha} + ik_{\gamma 2}n_j v_k^{\gamma}\right]$$

and v_0 is the uniform velocity on the transducer surface, ρ_1,ρ_2 are the densities of the fluid and solid, respectively, ω is the circular frequency, and $k_{p1},k_{\gamma 2}$ (γ = P,S) are the wavenumbers associated with the first and second media, respectively. The material wavespeeds of the second medium are $c_{\gamma 2},c_{\alpha 2}$, and $T_{12}^{\alpha;P}$ is the plane wave transmission coefficient (based on pressure-stress ratios). C_{klij} is the fourth order tensor of elastic constants, d_i^{α} are the polarization components, n_k are the interface unit normal components, e_j^{α} are the components of a unit vector in the transmitted wave direction that satisfies Snell's law, f_{ln}^{γ} is a coefficient dependent on v_k^{γ} is a unit vector from the point $\mathbf{x}_s$ on the interface surface to the field point $\mathbf{x}_2$ in the second medium.

Equation (1) is called the Kirchhoff Beam Transmission (KBT) model. Because there are two surface integrations that must be performed, this particular model is quite cumbersome to numerically evaluate in its present state. One possible way to simplify this numerical evaluation is to apply the edge element method [7] to both transducer and interface surface integrals. This method divides both surfaces into a series of small, planar facets, where the amplitude term in Eq. (1) assumed to be constant over each facet and the phase is approximated to first order over each of the facets. The first order phase approximation allows Stokes' theorem to be applied to the surface integral associated with each planar facet, reducing the 2-D integral of that facet to a 1-D contour integral around the edge of the facet. The resulting 1-D line integration can be evaluated analytically if the edges of the facet are straight lines, resulting in a finite sum of sinc functions, where each term in the sum corresponds to a contribution from a particular edge of the facet being evaluated. Thus, a 2-D surface integral can be reduced to two nested finite summations, where one summation extends over the planar facets that represent the surface of integration, and the other summation accounts for the edge contributions of each individual facet. When applied to the KBT model, the edge element technique effectively reduces the two surface integrals to four finite sums, and the explicit form becomes

$$u_{Tn}^{\gamma}(\mathbf{x}_2,\omega) = \frac{\rho_1 c_{p1} v_0}{8\pi^2\rho_2\omega}\sum_{\alpha=P,S}\sum_{m=1}^{M}\sum_{q=1}^{Q}\sum_{s=1}^{S}\sum_{r=1}^{R}\frac{T_{12}^{\alpha;P}\left(\Theta_{10}^{mq}\right)}{r_{10}^{mq}r_{20}^{q}\left|\mathbf{p}_{\gamma 0}^{mq}\right|} I_n^{\alpha\gamma;mq}\exp\left[i\left(k_{p1}r_{10}^{mq}+k_{\gamma 2}r_{20}^{q}\right)\right] I_{mqs}^{T} I_{mqr}^{I;\gamma} \qquad (2)$$

where

$$\mathbf{p}_{\gamma 0}^{mq} = k_{p1}\mathbf{e}_{10}^{mq} - k_{\gamma 2}\mathbf{e}_{20}^{q}$$

and r_{10} is the distance between the mth transducer facet centroid and qth interface facet centroid, and r_{20} is the distance between the qth interface facet centroid and the field point, $\mathbf{x}_2$. $\mathbf{e}_{10}$ and $\mathbf{e}_{20}$ are the unit vectors associated with r_{10} and r_{20}, respectively. M (Q) and S (R) are

the total number of planar facets (and edges) of each facet, respectively, for the transducer (interface) surface, and I^{T}_{mqs}, $I^{I;\gamma}_{mqr}$ are modified sinc terms [7]. Although its computational speed will be faster than the original KBT model, the edge element method in Eq. (2) is still quite computationally intensive since both surfaces are typically discretized with hundreds of facets. However, complex surface geometries can be easily modeled because of the versatility of using an approach based on facets.

Another approach to simplifying the form of the KBT model involves explicitly evaluating the interface integral by invoking the method of stationary phase, leaving only the transducer surface integral to be performed numerically. The end result of this approach is the Surface Integral (SI) model. By expanding the phase term in Eq. (1) to second order along the stationary phase ray path (Snell's law ray path) and assuming the amplitude term in Eq. (1) remains constant and is equal to the amplitude along this ray path, the interface integral can be approximated with the method of stationary phase [7]. After some algebra, the displacement wavefields become

$$u^{\gamma}_{Tn}(\mathbf{x}_2,\omega) = \frac{i\rho_1 v_0}{2\pi\rho_2 c_{\gamma 2}} \int_{S_T} \frac{T^{\gamma;P}_{12} d^{\gamma}_n \exp[ik_{p1}r^{\gamma}_{10} + ik_{\gamma 2}r^{\gamma}_{20} + i\sigma^{\gamma}]}{r^{\gamma}_{10} r^{\gamma}_{20} \left[\left|\phi^{\gamma}_{p1}\right|\left|\phi^{\gamma}_{p2}\right|\right]^{1/2}} dS \qquad (\gamma = P,S) \qquad (3)$$

where

$$\sigma^{\gamma} = \pi(sgn\phi^{\gamma}_{p1} + sgn\phi^{\gamma}_{p2})/4$$

and $\phi^{\gamma}_{p1}, \phi^{\gamma}_{p2}$ are the principal values of a 2-D tensor, whose components are dependent upon the two principal radii of curvature (R_1, R_2) of the interface (for explicit expressions, see Schmerr et al. [8]). The remaining surface integral over the transducer face can be evaluated with edge elements or a numerical technique of the user's choice. Since the 2-D integral associated with the interface has been effectively eliminated by the stationary phase approximation, the SI model is much more computationally efficient when compared to either the KBT model or edge element model. However, the SI model will break down in caustic regions of focusing interfaces because it is inherently based on a ray path expansion. Corrections to the SI model could be made for these particular regions, but it is often simpler to just return to the edge element model or the original KBT model.

The SI model can be further simplified by reducing the 2-D transducer surface integral to a 1-D line integral around the extended edge of the transducer through the use of the paraxial approximation. The resulting model, called the paraxial boundary diffraction wave (PBDW) model, is a generalization of earlier paraxial models developed for planar interfaces [9] since the current model takes into account the effects of the interface curvatures on the transmitted displacement fields. The PBDW expression can be found by expanding the phase term of the SI model to second order about a fixed ray path traveling normally from the transducer surface to the field point of evaluation in the second medium, and assuming the amplitude terms are taken as their constant values along this ray path. The resulting surface integral can be written in terms of polar coordinates, and because of the second order phase approximation, the radial component of the integral can be integrated exactly, leaving only the angular integral to be evaluated numerically. As a result, the displacements in the solid become

$$u^{\gamma}_{n}(\mathbf{x}_2,\omega) = \frac{\rho_1 c_1 v_0}{i\omega\rho_2 c_{\gamma 2}} T^{\gamma;P}_{12} d^{\gamma}_n \exp\left[i\left(k_1 D^{\gamma}_{10} + k_{\gamma 2} D^{\gamma}_{20}\right)\right] C^{\gamma}_1(S_T,\omega) \qquad \gamma = P,S \qquad (4)$$

where the diffraction coefficient, $C^{\gamma}_1(S_T,\omega)$, is given by

$$C^{\gamma}_1(S_T,\omega) = \frac{-i\exp(i\sigma^{\gamma})}{2\pi D^{\gamma}_{10} D^{\gamma}_{20}\left[\left|\phi^{\gamma}_{p1}\right|\left|\phi^{\gamma}_{p2}\right|\right]^{1/2}} \int_C \frac{\Theta^{\gamma} - \exp(ik_1\rho^2_e g^{\gamma}(\phi)/2)}{g^{\gamma}(\phi)} d\phi$$

and Θ and $g(\phi)$ are given explicitly in [8], D_{10}^{γ} and D_{20}^{γ} are the ray paths in the first and second media, respectively, and ρ_e is the radius from the origin of the fixed ray to the edge of the transducer. The PBDW model is extremely efficient to calculate, making it an excellent candidate for use in real-time ultrasonic inspection simulators. However, as with the SI model, this model will become singular at caustic regions. Also, the paraxial approximation will reduce its accuracy in the nearfield regions of the transducer.

COMPARISONS

Two sets of comparisons will be made. First, on-axis displacement profiles will be computed with the edge elements approach (Eq. (2)) for cylindrically converging and diverging interfaces, where the radii of curvature are ± 2". These edge element profiles will be compared to their more approximate PBDW paraxial counterparts (Eq. (4) in order to determine under what conditions the paraxial assumption can be invoked without sacrificing significant amounts of accuracy in the wavefield predictions. Next, the edge elements approach will be used to study three different, yet related, interface geometries by plotting each of their cross-axis profiles. A 2-D field image of the predicted wavefield for the fillet geometry (cylindrical interface located on one side of the transducer central axis, planar interface located on the other side) is also included.

The normalized incident displacement wavefields resulting from a unfocused, circular transducer radiating through a cylindrical fluid- solid interface are predicted by two of the models in Eqs. (2) and (4). Both models compute the phase and amplitude of the displacement at discrete spatial point in the wavefield, however, only the amplitudes predicted by the models will be compared here. The two media modeled are water (c_1 =1480 m/s) and steel (c_{p2}=5900 m/s). The comparisons will be restricted to on-axis profiles in the elastic solid, where the relative magnitudes of the displacements will be plotted against the z distance ($z = z_1 + z_2$) from the transducer face. The displacements will computed at a single, arbitrary frequency, taken here as the center frequency of the transducer.

The transducer to be modeled is a 1/2" dia., 5 MHz, unfocused probe which resides 2 cm (z_1 distance) from the cylindrical interface. For the comparisons shown here, the paraxial model used 128 line elements to represent the edge of the transducer. The edge element model discretized the transducer surface into approximately 800 area facets. The cylindrical interface requires no discretization in the paraxial model, however, for the edge element model, 676 area facets (26x26) are used on a 5 transducer radii by 5 transducer radii patch centered about the transducer's central axis.

Figures 2 and 3 show the on-axis incident displacement comparisons for the diverging and converging cylindrically focused, water-steel interfaces. As expected, the defocusing effect of the diverging interface reduces the predicted amplitudes significantly below planar interface amplitudes, while the converging interface produces the opposite effect by increasing the predicted amplitudes to values higher than planar interface amplitudes. The PBDW model is in excellent agreement with the edge element model throughout the entire profile plotted for the diverging interface case in Figure 2. However, for the converging interface case in Figure 3, the PBDW model becomes less accurate near the main peak of the profile.

Figure 4 shows the cross-axis profiles computed by edge elements of three related interface geometries: planar, filleted, and cylindrically focused (6" radius of curvature). The planar and cylindrically focused profiles are symmetric about the central axis, with peak amplitudes occurring on the central axis. However, the filleted interface profile is quite asymmetric, with its peak amplitude occurring slightly off the central axis on the planar side of the interface. Simple ray tracing from the transducer surface through the filleted interface predicts this type of behavior. Figure 5 displays a gray scale 2-D image of the ultrasonic beam propagating through the filleted interface, where the cylindrical portion (6" radius of curvature) of the interface is located above the central axis and the planar portion is locate below the central axis. As with the cross axis profile, no symmetry is seen in this

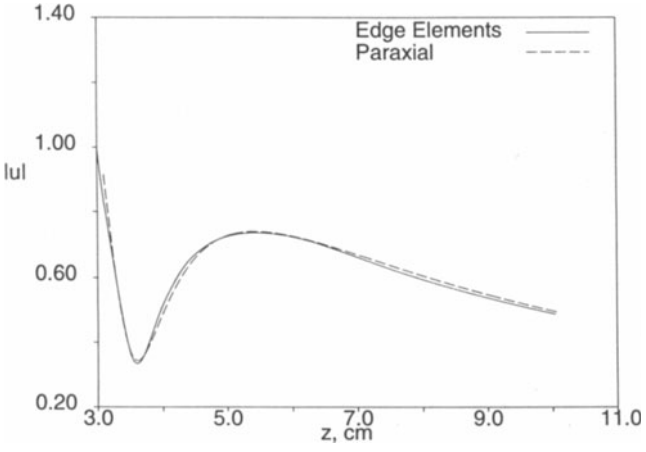

Figure 2. On-axis P-wave displacement profiles for a diverging, cylindrical, water-steel interface of 2" curvature and 2 cm waterpath (z1 distance). The z distance is equal to the sum of the waterpath and z2 distances.

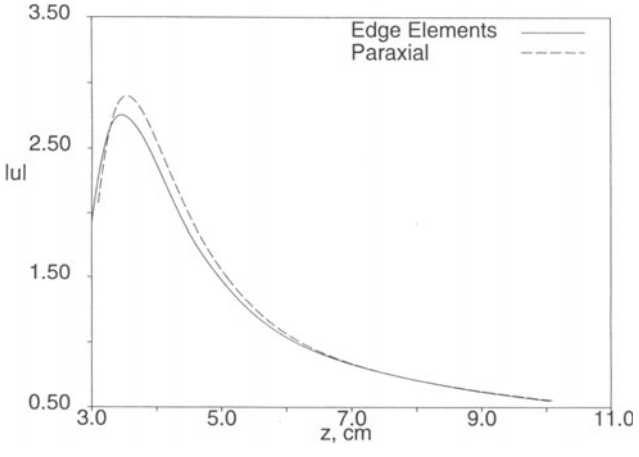

Figure 3. On-axis P-wave displacement profiles for a converging, cylindrical, water-steel interface of 2" curvature and 2 cm waterpath (z1 distance). The z distance is equal to the sum of the waterpath and z2 distances.

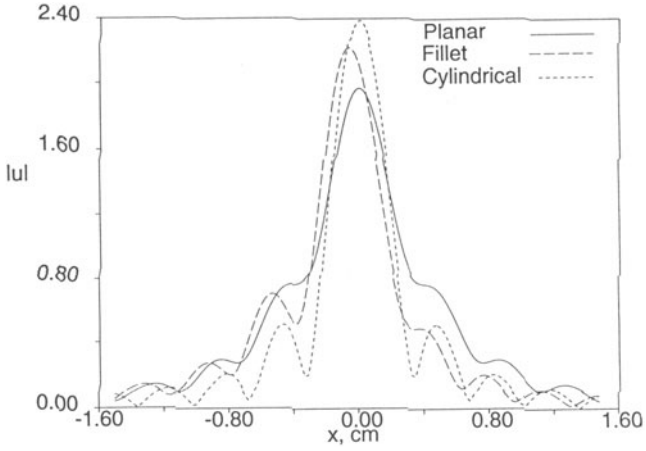

Figure 4. Cross-axis P-wave displacement profiles of 3 related interface geometries taken 3.1 cm (z2 distance) below the interface. The water path remains at 2 cm.

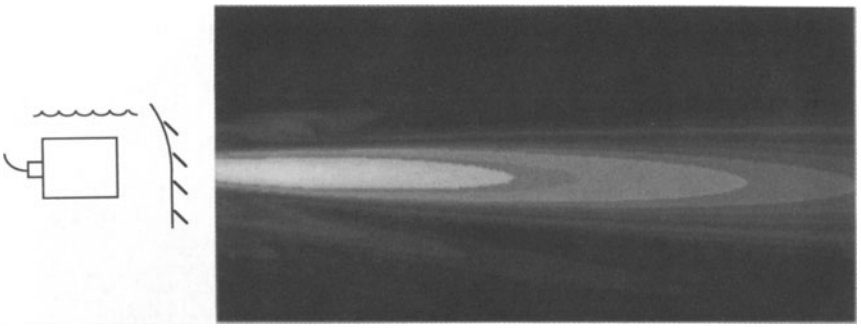

Figure 5. P-wave displacement wavefield transmitted through a filleted, water-steel interface with water path of 2". The image area (7cm x 3cm) is centered about the transducer's central axis and starts 2 cm deep into the steel. (Not to scale.)

image. The main and side lobes of the beam are skewed slightly towards the metal directly under the planar portion of the interface, just as ray tracing would qualitatively predict.

CONCLUSIONS

Four models developed for the transmission of ultrasonic radiation through curved, fluid-solid interfaces are briefly reviewed and comparisons of two of these models (PBDW and edge elements) are made. For the cases shown (and many others not included here), we find the PBDW paraxial based model is very accurate for planar and cylindrically defocusing interfaces throughout the majority of the wavefield (nearfield regions may become less accurate as the defocusing becomes slighter). However, the PBDW model tends to become less accurate, especially in nearfield and peak regions, as positive (converging) radii of curvature become more tightly focused.

The great benefit of the PBDW model is its computational speed; this model is approximately 2-3 orders of magnitude faster than the equivalent edge element model. Unfortunately, as with most ray-based models, the PBDW and SI models break down in caustic regions of the wavefield and require corrective measures at these locations. While the edge element and KBT models are much slower to compute, they can accommodate general interface geometries quite easily and do not fail at caustics or focal points.

ACKNOWLEDGMENTS

T. Lerch and L. Schmerr were supported in this work by the Program for Integrated Design, NDE, and the Manufacturing Sciences under U.S. Dept. of Commerce, National Institute of Standards and Technology Cooperative Agreement No. 70NANB4H1535. A. Sedov was supported by the Natural Sciences and Engineering Research Council of Canada.

REFERENCES

1. Thompson, R.B. and T.A. Gray, "A Model Relating Ultrasonic Scattering Measurements Through Liquid-Solid Interfaces to Unbounded Medium Scattering Amplitudes", *J. Acoust. Soc. Am.*, 74, 1279-1290, 1983.
2. Thompson, R.B., and E.F. Lopes, "The effects of focusing and refraction on Gaussian ultrasonic beams," *J. Nondestr. Eval.*, 4 (2), 107-123, 1984.
3. Newberry, B.P., Gray, T.A., Lopes, E.F., and R.B. Thompson, "Evaluation of ultrasonic beam models for the case of a piston transducer radiating through a liquid-solid interface," *Review of Progress in QNDE,* D.O. Thompson and D.E. Chimenti, Eds., Plenum Press, N.Y., 5A, 127-138, 1986.
4. Goswami, P.P., Rudolphi, T.J., Roberts, R.R., and F.J. Rizzo, "Ultrasonic transmission through a curved interface by boundary element method," *Review of Progress in QNDE,* D.O. Thompson and D.E. Chimenti, Eds., Plenum Press, N.Y., 10A, 193-200, 1991.
5. Zeroug, S., and L.B. Felsen, "Nonspecular reflection of two- and three-dimensional acoustic beams from fluid-immersed cylindrically layered elastic structures," *J. Acoust. Soc. Am.*, 98 (1), 584-598, 1995.
6. H.T. O'Neil, "Theory of focusing radiators," *J. Acoust. Soc. Am.*, 21, 516-526, 1949.
7. T. P. Lerch, "Ultrasonic transducer characterization and transducer beam modeling for applications in nondestructive evaluation", Ph.D. Dissertation, Iowa State University, 1996.
8. Schmerr, L.W., Lerch, T.P., and A. Sedov, "Modeling the propagation of bounded beams through curved interfaces," *Review of Progress in QNDE,* D.O. Thompson and D.E. Chimenti, Eds., Plenum Press, N.Y., 16, 845-851, 1997.
9. Lerch, T.P., Schmerr, L.W. and A. Sedov, "The Paraxial Approximation for Radiation of a Planar Ultrasonic Transducer at Oblique Incidence Through an Interface", *Review of Progress in QNDE,* D.O. Thompson and D.E. Chimenti, Eds., Plenum Press, N.Y., 14A, 1067-74, 1995.